

12-25-2014

Real-time Kinetic Studies of Bacillus Subtilis Oxalate Decarboxylase and Ceriporiopsis Subvermispora Oxalate Oxidase Using Luminescent Oxygen Sensor

Laura Molina
University of Florida

Thomas Goodall
University of Florida

Umar Twahir
University of Florida

Ellen W. Moomaw
Kennesaw State University, emoomaw@kennesaw.edu

Follow this and additional works at: <http://digitalcommons.kennesaw.edu/facpubs>

 Part of the [Biochemistry Commons](#), and the [Chemistry Commons](#)

Recommended Citation

Molina, Laura; Goodall, Thomas; Twahir, Umar; and Moomaw, Ellen W., "Real-time Kinetic Studies of Bacillus Subtilis Oxalate Decarboxylase and Ceriporiopsis Subvermispora Oxalate Oxidase Using Luminescent Oxygen Sensor" (2014). *Faculty Publications*. Paper 3718.

<http://digitalcommons.kennesaw.edu/facpubs/3718>

This Article is brought to you for free and open access by DigitalCommons@Kennesaw State University. It has been accepted for inclusion in Faculty Publications by an authorized administrator of DigitalCommons@Kennesaw State University. For more information, please contact digitalcommons@kennesaw.edu.

Real-Time kinetic studies of *Bacillus subtilis* oxalate decarboxylase and *Ceriporiopsis subvermispota* oxalate oxidase using a luminescent oxygen sensor

Laura Molina, Thomas Goodall, Umar Twahir, Ellen Moomaw, Alexander Angerhofer*

Received: 17 October 2014 / Received in revised form: 19 December 2014, Accepted: 19 December 2014,
Published online: 25 December 2014 © Biochemical Technology Society 2014

Abstract

Oxalate decarboxylase (OxDC), an enzyme of the bicupin superfamily, catalyzes the decomposition of oxalate into carbon dioxide and formate at an optimal pH of 4.3 in the presence of oxygen. However, about 0.2% of all reactions occur through an oxidase mechanism that consumes oxygen while producing two equivalents of carbon dioxide and one equivalent of hydrogen peroxide. The kinetics of oxidase activity were studied by measuring the consumption of dissolved oxygen over time using a luminescent oxygen sensor. We describe the implementation of and improvements to the oxygen consumption assay. The oxidase activity of wild type OxDC was compared to that of the T165V OxDC mutant, which contains an impaired flexible loop covering the active site. The effects of various carboxylic acid-based buffers on the rate of oxidase activity were also studied. These results were compared to the oxidase activity of oxalate oxidase (OxOx), a similar bicupin enzyme that only carries out oxalate oxidation. The temperature dependence of oxidase activity was analyzed, and preliminary results offer an estimate for the overall activation energy of the oxidase reaction within OxDC. The data reported here thus provide insights into the mechanism of the oxidase activity of OxDC.

Keywords: Enzyme kinetics, oxygen consumption, oxidase, decarboxylase

Introduction

Oxalate decarboxylase (OxDC), derived from the soil bacterium *Bacillus subtilis*, catalyzes the decomposition of oxalate into carbon dioxide and formate at an optimal pH of 4.3 in the presence of

Laura Molina, Thomas Goodall, Umar Twahir, Alexander Angerhofer*

Department of Chemistry, University of Florida, PO Box 117200,
Gainesville, FL 32611-7200

Tel: 352-392-9489; *Email: alex@chem.ufl.edu

Ellen Moomaw

Department of Chemistry and Biochemistry, Kennesaw State
University, 1000 Chastain Road, MD# 1203, Kennesaw, GA 30144

oxygen (Svedružić et al. 2005; Tanner et al. 2001). However, about 0.2% of all turn-over reactions occur through an oxidative mechanism that consumes one equivalent of dissolved dioxygen per oxalate while producing two equivalents of carbon dioxide and one hydrogen peroxide, as in the structurally similar enzyme oxalate oxidase derived from *Ceriporiopsis subvermispota* (OxOx) (Aguilar et al. 1999; Escutia et al. 2005). The overall reaction schemes are shown in Figure 1. Essentially, OxDC can follow two distinctly different chemical pathways using the same substrate. Dioxygen plays the role of a co-catalyst in the decarboxylation reaction and a co-substrate in the oxidation reaction.

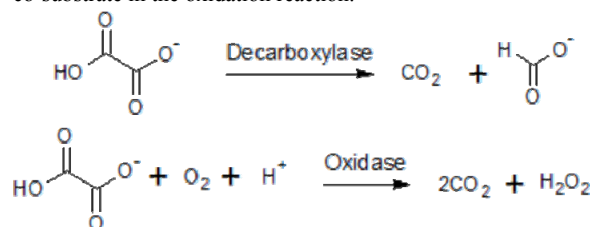


Figure 1: Overall reaction schemes describing the decomposition of oxalate by OxDC (Svedružić et al. 2005)

The active form of OxDC consists of a dimer of trimers (one trimer is shown in Figure 2), and each monomeric subunit contains two β -barrel domains holding a Mn (II). However, only the N-terminal Mn is suspected to form the active site where oxalate can bind, due to the presence of a small flexible amino acid loop SENST 161-5 (Anand et al. 2002; Just et al. 2007). Based on several crystal structures of OxDC, this loop may undergo conformational changes to open a solvent channel leading to the N-terminal Mn, allowing oxalate to enter the active site and bind to the Mn ion (Anand et al. 2002; Just et al. 2007). When the loops adopt a closed conformation over the active site, as shown in Figure 3, the Glu 162 residue comes into close proximity with the bound oxalate molecule and is hypothesized to undergo proton-coupled electron transfer essential for decarboxylase activity, as described in the proposed mechanism shown in Figure 4. Removal of the Glu 162 residue has been shown to drastically reduce decarboxylase activity while increasing oxidase activity (Burrell et al. 2007).

In order to further characterize the importance of the flexible loop SENST 161-5, the oxidase activity of the T165V mutant of OxDC was studied. The T165V mutation removes a hydrogen bond between T165 and R92, thereby reducing the stability of the closed loop conformation and presumably favoring the open over the closed conformation in solution (Imaram et al. 2011).

Previous studies determined that the overall enzymatic rate of T165V was reduced by almost a factor of 10 compared to WT OxDC, but the amount of oxidase activity was reduced only by about a factor of three, resulting in a factor of three enhancement of oxidase activity relative to decarboxylase activity in this mutant (Saylor et al. 2012).

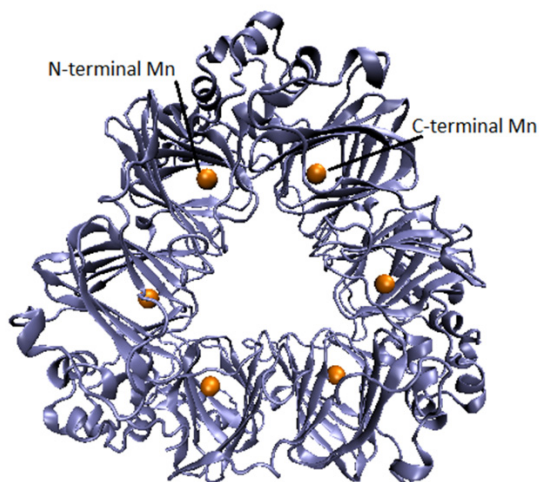


Figure 2: Crystal structure showing one of the two trimers that forms biologically active OxDC (Anand et al. 2002)

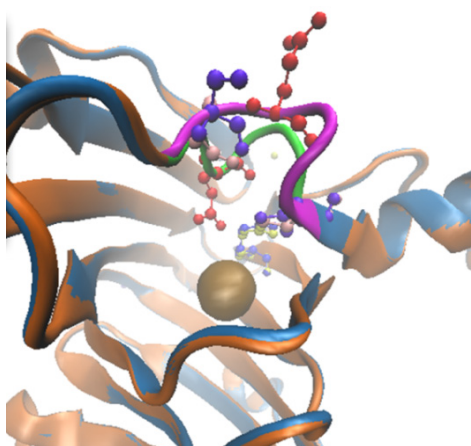


Figure 3: Flexible loop in its open (magenta) and closed (green) conformations. Glu162 is shown as a red ball-and-stick model, with the Mn atom shown in bronze. The blue protein chains correspond to the open crystal structure, while the orange protein chains correspond to the closed crystal structure.

In addition to measuring the oxidase activity of WT OxDC and the T165V mutant, the oxidase activity of WT oxalate oxidase (OxOx) was studied to provide a standard for comparison. Experiments were also carried out to study the temperature dependence of the oxidase activity of OxDC. An Arrhenius analysis provides an estimate of the activation energy of the oxidase reaction, which is similar to reported values for the activation energy of OxOx (Pundir 1993; Pundir et al. 1993). Finally, the choice of buffer was revealed to

significantly impact the reaction kinetics oxidase activity for both WT OxOx and OxDC. The effects of the carboxylic acid-based buffers acetate, citrate, and succinate were observed.

All of these studies of oxidase activity were carried out using a novel assay that measures oxygen consumption in real time. The oxidase activity of OxDC and OxOx had previously been measured using a continuous assay that coupled the production of H_2O_2 to the oxidation of 2,2'-azino-bis(3-ethylbenzothiazoline-6-sulphonic acid) (ABTS) by horseradish peroxidase (Moussatche et al. 2011). The absorbance of the radical products of ABTS at 650 nm was monitored to follow the progress of the reaction (Moussatche et al. 2011; Requena et al. 1999). The production of oxygen and CO_2 has also been monitored in real time using membrane inlet mass spectrometry (Moomaw 2014). In this paper, we describe a real-time assay that follows the consumption of dissolved oxygen, providing a direct measurement of oxidase activity without the potential errors introduced by using a secondary detection system as in the coupled assay. Initial experiments by our group using the new assay have already been reported (Saylor et al. 2012). Here we present a more detailed explanation of the assay protocol and improvements made by the addition of a temperature controller, resulting in an increase in the signal-to-noise ratio of the raw data.

Materials and methods

Enzyme Preparation

The expression and purification of OxDC and T165V were carried out using an *E. coli* expression system as described by Imaram, et al., and Saylor et al.(2011; 2012). The expression and purification of OxOx from *Ceriporiopsis subvermispora* was carried out using a *Pichia pastoris* expression system as described by Moussatche et al.(2011). Samples were kept at $-80^\circ C$ until ready for use.

Kinetic Assay of Oxidase Activity

Oxygen consumption for each enzyme preparation was measured using a NeoFox® Phase Measurement System from Ocean Optics, Dunedin, Florida, using the FOSPOR Oxygen Sensor formulation under controlled conditions. Dissolved oxygen concentration was measured using a Redeye® patch placed in solution, consisting of a FOSPOR ruthenium compound embedded in a sol-gel matrix. The ruthenium compound was excited using blue light from an LED through a fiber-optic cable, and the resulting luminescence was detected through the same cable. The red phosphorescence is quenched in the presence of oxygen, so the measurement of its intensity and lifetime served as a measure of the concentration of dissolved oxygen. Before conducting each series of reactions, the probe was calibrated under normal atmospheric conditions as well as under anoxic conditions after the cuvette was flushed with N_2 or Ar gas.

Reaction mixtures contained between 0.075 and 7.00 μM of either WT OxDC or T165V as well as oxalate concentrations ranging from 0.125 mM to 200 mM, with a total reaction volume of 2 mL. Oxalate solutions were prepared by weighing out the desired amounts of $K_2C_2O_4 \cdot H_2O$ (Sigma Aldrich) using a Fisher Science Education ALF64 analytical balance, and dissolving it in buffer solution at pH 4.3. Measurements on WT and T165V OxDC were performed in 0.5 M acetate or

succinate buffers. Since acetate has been shown to inhibit the activity of WT OxOx, 0.5 M citrate and 0.35 M succinate buffers were used for reactions with OxOx (Moussatche et al. 2011). Reactions were conducted in triplicate for each concentration of oxalate. The decrease in dissolved oxygen concentration was monitored as a function of time in order to measure the initial rate of reaction. An example reaction trace is shown in Figure 5.

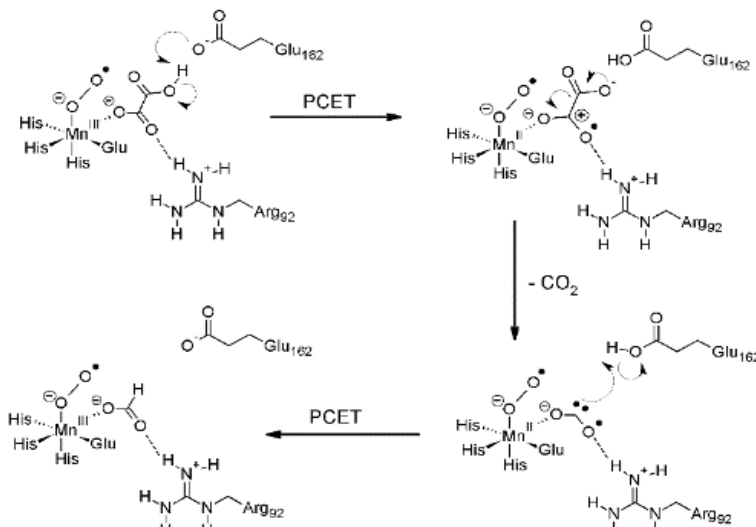


Figure 4: Proposed mechanism of decarboxylase activity of OxDC, showing proton-coupled electron transfer catalyzed by Glu162

Oxidase activity was defined as the initial rate of change of dissolved oxygen concentration over time, as taken from the linear portion of each reaction trace. A magnetic stir bar was used to ensure even mixing of the reactants and increase the signal-to-noise ratio throughout the experiment. The cuvette was tightly sealed with an o-ring, and in order to start the reaction, enzyme solution was injected through 1/16" Peek tubing attached to luer-lock connectors. The syringes remained attached to the luer-lock connectors throughout the experiment to prevent accidental leakage of atmospheric oxygen into the solution. Despite these precautions, small leaks were observed through the syringes while conducting experiments, most likely due to a sudden buildup of pressure, especially after solutions were injected into the cuvette. Although the effect of these leaks was usually small, the rate of oxygen consumption was corrected when necessary for the rate of oxygen reentry.

For temperature-dependent measurements, an Ocean Optics qpod 2e™ was used. This device is a temperature-regulated, Peltier-controlled cuvette holder that is able to control the temperature of a standard 1-cm square cuvette to $\pm 0.05^\circ\text{C}$. The qpod 2e™ also provides variable-speed magnetic stirring. It contains a horizontal opening allowing the Neofox oxygen sensor to reach the exterior of one side of the cuvette with minimal light intrusion, while the Redeye® ruthenium patch is placed on the corresponding inside wall of the cuvette. The cuvette was kept sealed using a similar arrangement as previously noted.

The temperature controller helped to enhance the signal-to-noise ratio when measuring the dissolved oxygen concentration over the course of each reaction with OxDC. With the improved setup, we were also able to measure the oxidase activity at oxalate concentrations as low as 0.125 mM with noise levels comparable to those detected at 5 mM oxalate without temperature control. The ability to analyze oxidase activity at lower substrate concentrations improved the accuracy of the Michaelis-Menten kinetic analysis by

better defining the shape of the curve at concentrations smaller than K_M .

Calculation of Kinetic Parameters

The concentration of dissolved oxygen was monitored over time using measurement intervals of 100 ms during the course

of each reaction. The initial rate of each reaction was taken as the slope of the linear portion of each graph (see Figure 7 for an example of raw data collected for WT OxDC). For each enzyme, the initial rates of reaction over a range of oxalate concentrations were measured in triplicate. A Michaelis-Menten analysis following Equation (1) was then performed on the data, relating the initial rate of reaction v to the concentration of oxalate $[S]$. Data was analyzed using KaleidaGraph (Synergy Software) non-linear curve fitting software.

$$v = \frac{V_{\max}[S]}{K_M + [S]} \quad (1)$$

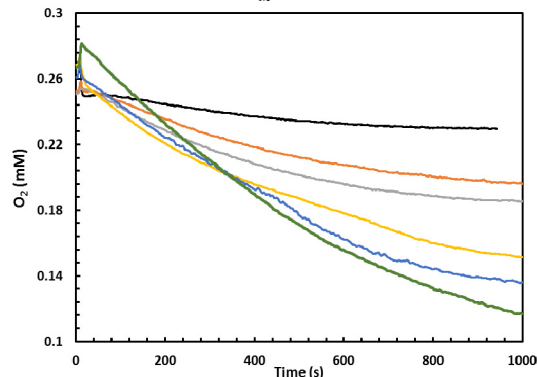


Figure 5: Sample set of raw experimental results, showing the concentration of dissolved oxygen over time during the reaction of WT OxDC over a range of oxalate concentrations: 5 mM (black), 10 mM (red), 20 mM (green), 50 mM (purple), 100 mM (blue), 200 mM (orange). Some variation is observed among the starting values of oxygen concentration after the calibration process. However, we are interested in a relative measure, observing the change of oxygen concentration over time. This reduces the impact of variation in the absolute values of dissolved oxygen concentration.

Results

The results yielded kinetic parameters characterizing the enzymes' oxidase activity and are recorded in Tables 1 and 2. Table 1 shows the effect of temperature on the oxidase activity of WT OxDC in succinate buffer. Table 2 compares the oxidase activities of WT OxDC, T165V OxDC, and WT OxOx under various buffer conditions.

Table 1: Temperature Dependence of the Kinetic Parameters of WT OxDC Oxidase Activity

WT OxDC	5°C	25°C	35°C
Enzyme Concentration [μM]	6.80 \pm 0.05	4.32 \pm 0.05	2.10 \pm 0.05
V_{max} [$\mu\text{M/s}$]	0.26 \pm 0.05	0.44 \pm 0.05	0.63 \pm 0.08
K_M [mM]	9.3 \pm 0.5	7.8 \pm 0.5	4 \pm 3
k_{cat} [s^{-1}]	0.04 \pm 0.02	0.10 \pm 0.02	0.30 \pm 0.04

Comparison of T165V with WT OxDC

The T165V mutant exhibited about the same oxidase activity as WT OxDC but with a slightly lower K_M than WT OxDC as shown in Figure 6. The improper closing of the loop thus appeared to enhance oxidase activity relative to decarboxylase activity. This is most likely due to the loss of control over the $\text{CO}_2^{\cdot-}$ radical intermediate into the solution which reacts with oxygen to form carbon dioxide and superoxide rather than more efficient oxygen binding to the mutant enzyme (Imaram et al. 2011). The decarboxylase activity of T165V has been observed to decline approximately ten-fold compared to WT OxDC which demonstrates the importance of the closed-loop conformation in the decarboxylase mechanism (Burrell et al. 2007).

Temperature Dependence of WT OxDC Oxidase Activity

The rate of oxidase activity of the WT enzyme was studied at 5, 25, and 35°C, and results show that the rate consistently increased with temperature, reaching significantly higher rates at 35°C (Table 1 and Figure 7). This result matches well with published observations of generally increased OxDC activity at 37°C (Lee et al. 2014). Based on the available data, a preliminary Arrhenius analysis (Figure 8) offers an estimate of the overall activation energy as 7.8 ± 0.4 kcal/mol. Considering that oxidase activity represents only a small fraction of the total activity of OxDC, it is interesting to note that the energy barrier for the oxidase reaction compares favorably to those previously reported for OxOx, ranging from 4 to 9 kcal/mol (Pundir 1993; Pundir, et al. 1993). This could mean that the mechanism for oxalate oxidation is the same in both types of enzymes.

Impact of Buffer on Oxidase Activity and Substrate-Dependent Inhibition

WT OxOx in succinate buffer showed 10x higher oxidase activity than in citrate buffer at the same pH, as demonstrated by the increased V_{max} and k_{cat} (see Figure 9). Citrate, along with acetate, thus appears to suppress enzymatic activity relative to succinate as described previously by Moussatche, et al. (2011). Interestingly, OxOx also demonstrates substrate-dependent inhibition at high oxalate concentrations (≥ 25 mM), where a decrease in activity of OxOx can be observed in the presence of both citrate and succinate buffers. While this effect has been previously observed in OxOx, it

remains to be explained, and it could be due to substrate and/or product inhibition or a secondary effect of oxalate on the enzyme, e.g., binding of oxalate to the C-terminal Mn (Pundir 1993).

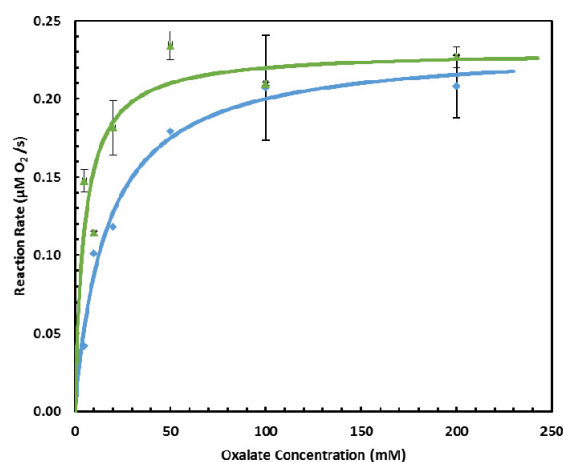


Figure 6: Comparison of Michaelis-Menten kinetic analysis of WT (blue) and T165V OxDC (green)

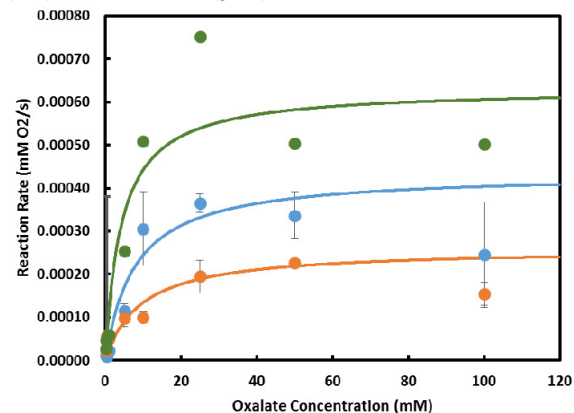


Figure 7: A comparison of the Michaelis-Menten kinetics of oxidase activity of OxDC at 5°C (orange), 25°C (blue), and 35°C (green).

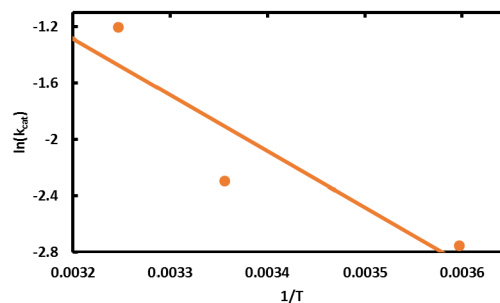


Figure 8: Arrhenius plot for WT OxDC Oxidase activity

WT OxDC shows no substrate-dependent inhibition of its oxidase activity in acetate buffer. However, in succinate buffer some substrate-dependent inhibition of oxidase activity is observed at high oxalate concentrations, as can be seen in Figure 10. This effect continues to be observed at 35°C, despite achieving a higher rate of oxidase activity at this temperature, as can be seen in Figure 9. Perhaps the enzyme has difficulty releasing products from the active site, which may have contributed to the observation of product in the

Table 2: Michaelis-Menten Parameters of Oxidase Activity (** Measured using temperature controller at 25°C)

	WT OxDC – Acetate Buffer	WT OxDC – Succinate Buffer**	T165V OxDC – Acetate Buffer	WT OxOx – Citrate Buffer	WT OxOx – Succinate Buffer
Enzyme Concentration [μM]	2.50 \pm 0.05	4.32 \pm 0.05	2.16 \pm 0.04	0.078 \pm 0.004	0.078 \pm 0.004
V_{max} [$\mu\text{M/s}$]	0.23 \pm 0.01	0.44 \pm 0.05	0.23 \pm 0.02	0.3 \pm 0.1 ₅	3.0 \pm 0.2
K_M [mM]	17 \pm 1	7.8 \pm 0.5	5 \pm 2	1.3 \pm 0.9	0.17 \pm 0.06
k_{cat} [s^{-1}]	0.093 \pm 0.005	0.10 \pm 0.02	0.10 \pm 0.01	4 \pm 2	39 \pm 4
k_{cat}/K_M [$\text{s}^{-1} \text{M}^{-1}$]	5.6 \pm 0.4	13 \pm 5	22 \pm 10	2700 \pm 2200	240,000 \pm 90000

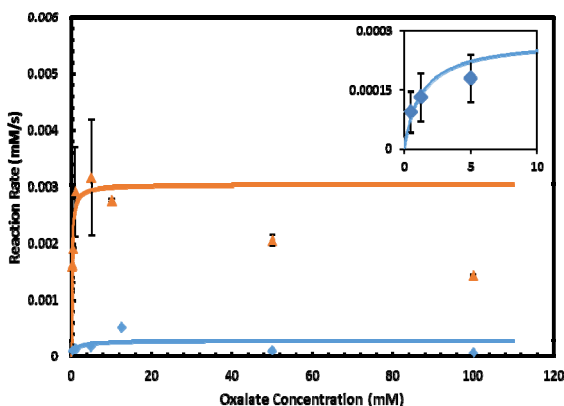


Figure 9: Buffer dependence of Michaelis-Menten Kinetics of WT Oxalate Oxidase in Succinate buffer (orange) or Citrate buffer (blue). Inset shows the kinetic profile of WT OxOx in citrate buffer between 0 and 10 mM oxalate for clarity.

N-terminal site in the original crystal structure by Anand et al. (2002). The optimum temperature of OxDC

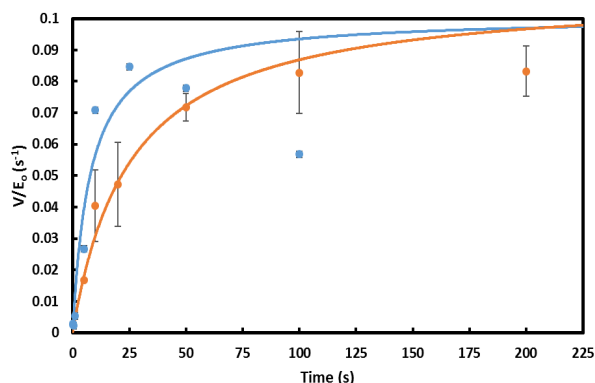


Figure 10: Comparing the Michaelis-Menten kinetic parameters of WT OxDC in acetate buffer at room temperature (orange) and WT OxDC in succinate buffer at 25°C (blue). The error bars for the blue data points are too small to be clearly distinguished.

was reported at around 35°C (Lee et al. 2014; Shady et al. 2013). This could indicate that comparisons between different enzymes should include measurements performed at higher temperatures.

When studying WT OxDC in succinate buffer, the reaction rates measured at 100 mM were not included in the calculation of kinetic parameters. This apparent inhibition must be examined carefully with a more detailed kinetic analysis to determine the type and extent of inhibition.

Discussion

Kinetic studies of OxDC and OxOx had previously relied on stopped end-point assays to measure the production of formate resulting from decarboxylase activity or the production of hydrogen peroxide resulting from oxidase activity (Burrell et al. 2007; Moussatche et al. 2011). The continuous assay based on oxygen consumption was only recently introduced as a new method to study the oxidase activity of these enzymes (Saylor et al. 2012). The results provide interesting insights into the oxidase activity of these enzymes.

In particular, these experiments help quantify the effect of the flexible amino acid “lid” in directing the bifurcation of the mechanism of OxDC. A reduction in the stability of the closed conformation of the active site has been shown to favor the oxidase mechanism of activity, as revealed by the T165V mutant, while in general reducing the activity of OxDC. It is still unknown whether oxidase activity proceeds via a bound oxygen molecule within the active site or through loss of the CO_2^- radical anion into the solution where it can subsequently react with dissolved O_2 to produce superoxide. At a pH below 5 where the enzyme is mainly active, superoxide would disproportionate rapidly into H_2O_2 and O_2 , leading to the observed oxidase activity (Finkelstein, et al. 1980).

An estimate of the activation energy of oxidase activity in WT OxDC shows that the magnitude of the reaction barrier is similar to that of other oxidase enzymes (Pundir 1993; Pundir, et al. 1993). Further studies of the OxDC mutants may reveal how the structural changes affect the energy barriers to both oxidase and decarboxylase activity. In addition, the comparison between OxDC and OxOx has revealed the possibility of inhibition of oxidase activity at high concentrations of oxalate as well as yet unexplained inhibitory effects of various buffers. These observations seem to be linked to the temperature dependence of WT OxDC, which requires further investigation. Finally, these experiments demonstrate the utility of the real-time assay following the consumption of dissolved oxygen over the course of each reaction. Overall, the collection of kinetic data provides important data for a more detailed explanation of the bifurcation of catalytic pathways in OxDC.

Acknowledgements

Funding for this project was provided to AA by the NSF (CHE-1213440). Funding was also provided by the National Science Foundation (MCB-1041912) to EWM. We are grateful to Dr. Nigel Richards, Indiana University Purdue University Indianapolis (IUPUI) for his continued interest in this project.

References

- Aguilar C, Urzúa U, Koenig C et al. (1999) Oxalate Oxidase from *Ceriporiopsis subvermispota*: Biochemical and Cytochemical Studies."Arch. Biochem. Biophys. 366.2:275–282.
- Anand R, Dorrestein PC, Kinsland Cet al. (2002) Structure of Oxalate Decarboxylase from *Bacillus Subtilis* at 1.75 Å Resolution. Biochem. 41.24: 7659–7669.
- Burrell MR, Just VJ, Bowater Let al. (2007) Oxalate Decarboxylase and Oxalate Oxidase Activities Can Be Interchanged with a Specificity Switch of up to 282 000 by Mutating an Active Site Lid. Biochem. 46.43: 12327–12336.
- Escutia MR, Bowater L, Edwards A et al. (2005) Cloning and Sequencing of Two *Ceriporiopsis subvermispota* Bicupin Oxalate Oxidase Allelic Isoforms: Implications for the Reaction Specificity of Oxalate Oxidases and Decarboxylases."Appl. Env. Microbiol. 71.7:3608–3616.
- Finkelstein E, Rosen GM, Rauckman EJ. (1980) Spin Trapping. Kinetics of the Reaction of Superoxide and Hydroxyl Radicals with Nitrones. JACS 102.15: 4994–4999.
- Imaram W, Saylor BT, Centonze CP et al. (2011) EPR Spin Trapping of an Oxalate-Derived Free Radical in the Oxalate Decarboxylase Reaction. Free Radical Bio Med 50.8: 1009–1015.
- Just VJ, Burrell MR, Bowater L et al. (2007) The Identity of the Active Site of Oxalate Decarboxylase and the Importance of the Stability of Active-Site Lid conformations. Biochem J 407.3: 397.
- Lee E, Jeong BC, Park YH et al. (2014) Expression of the Gene Encoding Oxalate Decarboxylase from *Bacillus Subtilis* and Characterization of the Recombinant Enzyme. BMC Research Notes 7.1: 598.
- Moomaw EW, Angerhofer A, Moussatche Pet al. (2009) Metal Dependence of Oxalate Decarboxylase Activity. Biochem 48.26: 6116–6125.
- Moomaw EW, Uberto R, Tu C. (2014) Membrane Inlet Mass Spectrometry Reveals That *Ceriporiopsis Subvermispota* Bicupin Oxalate Oxidase Is Inhibited by Nitric Oxide. Biochem Bioph Res Co 450.1: 750–754.
- Moussatche P, Angerhofer A, Imaram Wet al. (2011) Characterization of *Ceriporiopsis Subvermispota* Bicupin Oxalate Oxidase Expressed in *Pichia Pastoris*. Arch Biochem and Biophys 509.1: 100–107.
- Pundir, CS (1993) Purification and Properties of an Oxalate Oxidase from Leaves of Grain Sorghum Hybrid CSH-5. BBA-Protein Struct M 1161.1: 1–5.
- Pundir, CS, Kuchhal NK, Satyapal (1993) Barley Oxalate Oxidase Immobilized on Zirconia-Coated Alkylamine Glass Using Glutaraldehyde. Indian J Biochem Bio 30.1: 54–57.
- Requena L, Bornemann S (1999) Barley (*Hordeum Vulgare*) Oxalate Oxidase Is a Manganese-Containing Enzyme. Biochemical J 343.Pt 1: 185–190.
- Saylor BT, Reinhardt LA, Lu Zet al.(2012) A Structural Element That Facilitates Proton-Coupled Electron Transfer in Oxalate Decarboxylase. Biochem 51.13: 2911–2920.
- Shady HA, Kilany M, Genedi Qet al. (2013) Purification, Characterization and Molecular Studies on Oxalate Decarboxylase from *B. Cepacia* Inhabits Egyptian Soil. Egypt Acad J Biol Sci 5.2: 77–86. Print.
- Svedružić D, Jónsson S, Toyota Cet al.(2005) The Enzymes of Oxalate Metabolism: Unexpected Structures and Mechanisms. Archives Biochem Bioph 433.1: 176–192.
- Tanner A, Bowater L, Fairhurst S A., et al. (2001) Oxalate Decarboxylase Requires Manganese and Dioxygen for Activity. Overexpression and Characterization of *Bacillus Subtilis* YvrK and YoaN. J Biol Chem 276.47: 43627–43634.